

RSC Advances



This is an *Accepted Manuscript*, which has been through the Royal Society of Chemistry peer review process and has been accepted for publication.

Accepted Manuscripts are published online shortly after acceptance, before technical editing, formatting and proof reading. Using this free service, authors can make their results available to the community, in citable form, before we publish the edited article. This *Accepted Manuscript* will be replaced by the edited, formatted and paginated article as soon as this is available.

You can find more information about *Accepted Manuscripts* in the [Information for Authors](#).

Please note that technical editing may introduce minor changes to the text and/or graphics, which may alter content. The journal's standard [Terms & Conditions](#) and the [Ethical guidelines](#) still apply. In no event shall the Royal Society of Chemistry be held responsible for any errors or omissions in this *Accepted Manuscript* or any consequences arising from the use of any information it contains.

COMMUNICATION

White Light Emitting Diodes Based on A Yellow Thermally Activated Delayed Fluorescent Emitter and Blue Fluorescent emitter

Cite this: DOI: 10.1039/x0xx00000x

Received 00th January 2012,
Accepted 00th January 2012

DOI: 10.1039/x0xx00000x

www.rsc.org/

Lingqiang Meng,^{a,b,c} Hui Wang,^{a,b,c} Xiaofang Wei,^{a,b,c} Xiaopeng Lv,^d Ying Wang^{a,b,*}
and Pengfei Wang^{a,b}

Multi-emissive layer white organic light-emitting diodes (WOLEDs) based on a blue fluorescent emitter and a yellow thermally activated delayed fluorescent emitter were constructed with the co-host of mCP. The WOLEDs afforded a color coordination of (0.34,0.34), low efficiency roll-off achieved, and a maximum external quantum efficiency of 4.7%.

White organic light emitting diodes (WOLEDs) are attracting much more attention in the past decades due to their potential application as the solid-state light source, backlights for liquid crystal displays (LCD), and full color OLEDs.¹⁻³ Several methods have been developed to realize stable WOLEDs with high efficiency, stable Commission Internationale de l'Eclairage coordinates (CIE), and acceptable Color rendition index (CRI) over 75, such as hybrid WOLEDs, and co-doping multiple phosphorescent emitters with different color in one emissive layer.⁴⁻⁸ High efficiency WOLEDs with a maximum power efficiency ($\eta_{p,max}$) of 59.9 lm/W, external quantum efficiency (EQE) and CRI over 80 have been reported by incorporating mer-tri(*N*-dibenzofuranyl-*N'*-methylimidazole)iridium(III) [Ir(dfbmi)] as a blue emitter and bis(2-phenylbenzothiazolato) (acetylacetonate)iridium(III) [BT₂Ir(acac)] as a yellow emitter.⁹ In these WOLEDs, the phosphors have become indispensable owing to their ability to efficient participation of both singlet and triplet excitons, achieving nearly 100% internal quantum efficiencies and then producing high efficiency WOLEDs. However, the phosphors are generally incorporated with noble metal in their molecular structure, inducing the high cost of the devices. Moreover, the stability of the phosphors are not very satisfied. Especially the blue phosphors are easily to loss their color fidelity, which finally causes the tough achievement of high efficiency, stable WOLEDs. While, WOLEDs with long lifetime can be achieved by the application of fluorescence due to their intrinsic stable properties.

Qiu *et al.* reported high efficiency WOLEDs based on fluorescent emitter with extremely long lifetime (14.7 cd/A, 3000 h at an initial brightness of 10000 cd/m²) by controlling the recombination zone utilizing a double blue emitting layer to stabilize the blue emission.¹⁰ Their efficiency are limited by the loss of triplet excitons during electrical excitation, and thus, the efficiency of WOLEDs are still not satisfied, and cannot be comparable with WOLEDs based on phosphors. Thus, further improvement of both efficiency and stability of WOLEDs is still a challenge for the development of future displays and lightings.

Recently, pure organic thermally activated delayed fluorescence (TADF) emitters were developed as the new high efficiency fluorescent emitters, which both singlet and triplet can be harvested for light emission to achieve close to 100% internal quantum efficiency by the spin up-conversion process from triplet state to singlet state.¹¹ Lee's group reported high efficiency hybrid WOLED combining a green TADF emitting material with red/blue phosphorescent emitting materials. A high EQE above 20% has been achieved in the hybrid WOLED, which is comparable to those of phosphorescent WOLEDs.¹² Thus, the TADF emitter have the great potential to be used as the emitters for high efficiency WOLEDs with excellent stability. Adachi's group pioneered the high efficient organic fluorescent WOLEDs based on TADF emitters. The WOLEDs with the maximum luminescence of 9800 cd/m² can be turn on at about 5 V, and the performance of the devices are among the highest of traditional pure organic fluorescent WOLEDs, with current efficiency of 16.7 cd/A, EQE of 6.7% and CIE of (0.32,0.39).¹³ Recently, they reported a white TADF-assisted fluorescence (TAF)-OLEDs with a high EQE of over 12% and CIE coordinates of (0.25, 0.31), which contains a blue TADF molecule as a common exciton donor and red/green classical fluorescent molecules as exciton acceptors.¹⁴ Nevertheless, the reported pure organic fluorescent WOLEDs are still rare, and the performance of the devices are still limited. The reported WOLEDs based on TADF

emitters always show high efficiency at very low current density and luminance, and cannot satisfy the application in display and lighting.

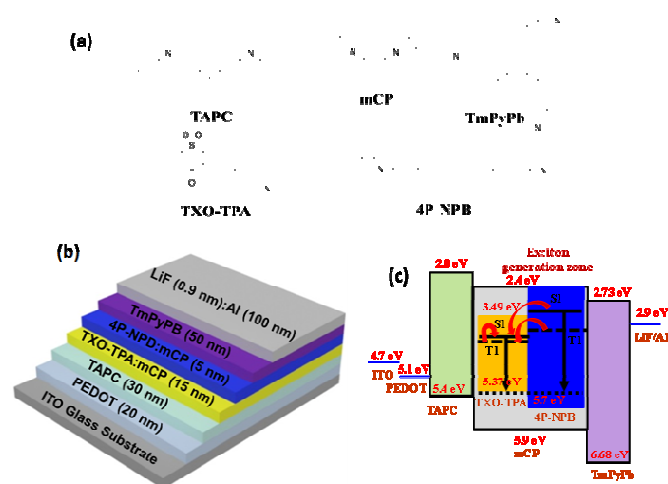


Figure 1. (a) The molecular structure of the materials used for the construction of WOLEDs; (b) Device structure and molecule arrangement of the WOLEDs; (c) Energy level scheme for materials used in the WOLEDs, and exciton energy diagram of the emitter layers.

Our group reported a novel TADF emitter of TXO-TPA, and the devices based on TXO-TPA gave yellow electroluminescence centred at 552 nm with color coordinates of CIE (0.45,0.53).¹⁵ The yellow OLEDs exhibited very high efficiency without any light out-coupling enhancement, and TXO-TPA can be possibly used for the construction of WOLED combining with blue fluorescent emitters. In this communication, high efficiency pure organic fluorescence WOLEDs were developed incorporating a yellow TADF emitter and blue fluorescent emitter. Two separated yellow and blue emitting layers were used for the fabrication of the pure organic fluorescent WOLEDs. The optimized device exhibits good EL performance with a turn-on voltage of 4 V. The maximum EQE, current efficiency and power efficiency of the device are 4.4%, 10.9 cd/A, and 8.5 lm/W, which are better than those of the WOLED base on pure fluorescent emitters.

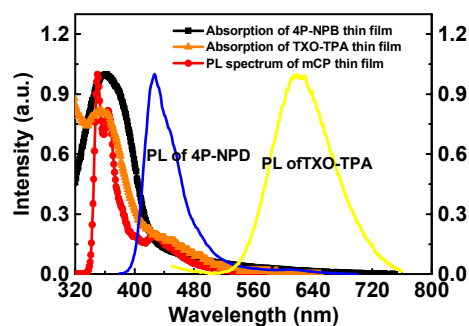


Figure 2. The absorbance of 4P-NPB and TXO-TPA in thin film, and the PL spectrum of mCP thin film.

To develop a high efficiency white OLED with high CRI, a blue emitter with high fluorescent quantum yield (η_{PL}) are indispensable. Here 4P-NPB was used as the fluorescent blue emitter due to its high η_{PL} of 92%. TXO-TPA was chosen as the orange dopant. mCP was chosen as the host for the reasons following: i) the high triplet

energy level to confine the triplet excitons on the emitters, ii) an appropriate ionization potential and electron affinity to adjust the carrier balance of holes and electrons in the emissive layer. In order to reduce the structural heterogeneity and facilitate charge transport between the two adjacent emitting layers, mCP was used as a common host for all lumophores. The device structure of the WOLEDs, the chemical structure and the energy level of the materials used are shown in Figure 1. As shown in Figure 1, these two primary-color emitters were arranged with a sequence of yellow-blue from the anode to the cathode. To transfer the energy of singlet excitons from mCP to 4P-NPB, a large spectral overlap between the ground state absorption of the exciton acceptor and fluorescent emission of the exciton donor is required. Figure 2 shows the absorption spectra of TXO-TPA and 4P-NPB and the PL spectrum of mCP. The film of mCP shows two sharp emission peaks centered at 364 and 350 nm with a long tail. Thin films of 4P-NPB exhibits a rather broad absorption peak with a full width at half-maximum of 82 nm and peak wavelength of 362 nm. Thus, singlet energy from mCP is expected to be transferred to S_1 of the 4P-NPB via a Förster process after the optically or electrically excitation of mCP molecules. Similar spectra overlap between the PL spectrum of mCP and the absorption of TXO-TPA can also be observed.

Excitons are formed on the mCP host with a singlet-to-triplet formation ratio (1:3). Singlet excitons are transferred following a Förster resonant process onto the doped blue fluorophore of 4P-NPB for blue light (as shown in Figure 2). While, the host triplets can migrate from the 4P-NPB:mCP layer to the TXO-TPA:mCP layer and efficiently transfer to the TXO-TPA by Dexter transfer process in that the non-radiative host triplets typically have long diffusion lengths (~100 nm). Thus, TXO-TPA can emit yellow light by the efficient up-conversion from triplet to singlet (as shown in Figure 2). Although there are some unavoidable loss in these transfer process, high efficient WOLEDs with the potential for unity internal quantum efficiency can be expected in the device structure since both singlet and triplet excitons can be utilized along independent channels. The balance of yellow emission and blue emission by the dedicate management of singlet and triplet excitons in the two emitting layers will be the key for the efficient WOLEDs (as shown in Figure 2).

Table 1. Electroluminescence characteristics of the OLEDs with different doping concentrations of 4P-NPB.

Doping Concentration of 4P-NPB	Maximum Values				Color Coordinate at 6 V
	Turn-on Voltage (V)	Current Efficiency (cd/A)	Power Efficiency (lm/W)	EQE (%)	
0.5%	3.9	9.0	4.7	3.3	(0.39,0.51)
2%	3.9	20.0	16.1	14.0	(0.37,0.42)
5%	3.8	15.5	12.6	7.5	(0.31,0.35)
10%	4	8.1	4.3	4.1	(0.30,0.33)
20%	3.9	5.2	3.3	3.0	(0.27,0.27)

As we had demonstrated high efficient yellow OLEDs based on TXO-TPA with the concentration of 5±1wt%, the TXO-TPA concentration will be kept in the yellow emitting layer here. We first optimized the concentration of 4P-NPB in the blue emission layer. The doping concentration of 4P-NPB was changed from 0.5% to 20%, and the performance of all devices with different doping

concentrations of 4P-NPB are summarized in Table 1. All these devices exhibited a turn-on voltage of 4 V. The device with a doping concentration of 0.5 wt% emits only yellow light with an emission peak of 552 nm and a color coordinate (0.39,0.51). With increasing the 4P-NPB concentration, the blue emission from 4P-NPB appears and the intensities of these peaks increase. The color coordinate shifts from yellow light region into white light region. Since mCP is a hole transporting materials with a high hole mobility of $1.2 \times 10^{-4} \text{ cm}^2/\text{Vs}$, which is three times higher than that of electron mobility ($4 \times 10^{-5} \text{ cm}^2/\text{Vs}$).¹⁶ And the hole mobility of 4P-NPB is also significantly higher than the electron mobility ($\mu_h = 6.6 \times 10^{-4} \text{ cm}^2/\text{Vs}$ and $\mu_e = 3.6 \times 10^{-8} \text{ cm}^2/\text{Vs}$).¹⁷ The exciton generation zone should be located at the 4P-NPB:mCP/TmPyPB interface. At the low doping concentration, the majority of the singlet excitons in the exciton generation zone will not decay on the 4P-NPB molecules, resulting in the blue emission. As the Förster distance of mCP and TXO-TPA is short, the singlet excitons also cannot effectively reach TXO-TPA via Förster resonant process and lead to the yellow emission. Thus, the efficiency of the device with the doping concentration of 0.5 wt% is inferior, markedly lower than that of OLEDs with only TXO-TPA as an emitter ($\eta_{\text{EQE}}=18\%$). When the doping concentration of 4P-NPB increases from 0.5 wt% to 2 wt%, the performance of the device remarkably increases due to the effective exploitation of the singlet excitons by 4P-NPB. While, the similar triplet energy of 4P-NPB (2.3 eV) compared to that of TXO-TPA (2.27 eV) leads to a possible Dexter energy transfer from the triplet state of TXO-TPA to the lower lying non-radiative triplet state of 4P-NPB, resulting in energy loss and thus a reduction in device efficiency. Thus, further increasing the doping concentration, the performance of the devices decrease because 4P-NPB can also be the trapping centers of triplet excitons. The device with a doping concentration of 2 wt% exhibits the highest performance with stable EL spectra, and the electroluminescence characteristics of the warm WOLEDs were shown in Figure 3. The device affords a current efficiency of 10.9 cd/A, a power efficiency of 8.5 lm/W, and EQE of 4.4%, which are comparable with those of the devices based on fluorescent and phosphorescent emitters with similar structure.³ As lighting sources are generally characterized by their total emitting power, the maximum total efficiencies of the devices can be up to 18.5 cd/A, 14.5 lm/W, and 7.5%. From EL spectrum, it is clear that the sufficient blue emission for the warm WOLEDs can be achieved at

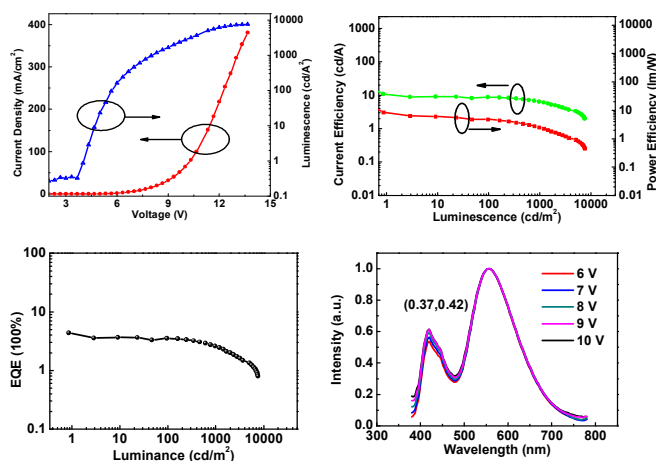


Figure 3. Electroluminescence characteristics of the OLEDs with a 4P-NPB doping concentration of 2 wt%: (a) Current density-voltage-luminance plots; (b) Current efficiency-luminance-power efficiency plots; (c) EQE-luminance plot; and (d) EL spectra of the device at different voltage.

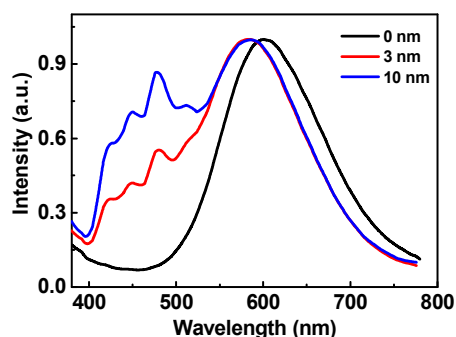


Figure 4. The normalized EL spectra for the devices with structure of ITO/PEDOT (20 nm)/TAPC (30 nm)/TPA (10 nm)/mCP (x nm)/4P-NPB (0.5 nm)/mCP (10 nm)/TmPyPB (50 nm)/LiF (0.9 nm)/Al (100 nm) (x = 0, 3, and 10 nm).

low concentration of 4P-NPB. Notably, the EL spectra are independent of the applied voltage and there were no derivation or new peaks even at high voltage up to 10 V. As the low doping concentration of 4P-NPB, the generated triplet excitons cannot be efficiently transfer to 4P-NPB by Dexter energy transfer process. Consequently, it can be inferred that the triplet excitons will diffused into the TXO-TPA:mCP layer. To further get the strong evidence for the diffusion of triplet excitons to the TXO-TPA:mCP layer, the devices with structure of ITO/PEDOT (20 nm)/TAPC (30 nm)/TPA (0.5 nm)/mCP (x nm)/4P-NPB (0.5 nm)/mCP (10 nm)/TmPyPB (50 nm)/LiF (0.9 nm)/Al (100 nm) (x = 0, 3, and 10 nm) were fabricated. When there is no spacer between TXO-TPA and 4P-NPB, there is barely the emission from TXO-TPA can be observed (as shown in Figure 4). Inserting a thin layer of mCP spacer, the emission from 4P-NPB appears and the intensity of the emission from 4P-NPB increases with the spacer thickness, providing a well-established proof for the diffusion (as shown in Figure 4).¹⁸

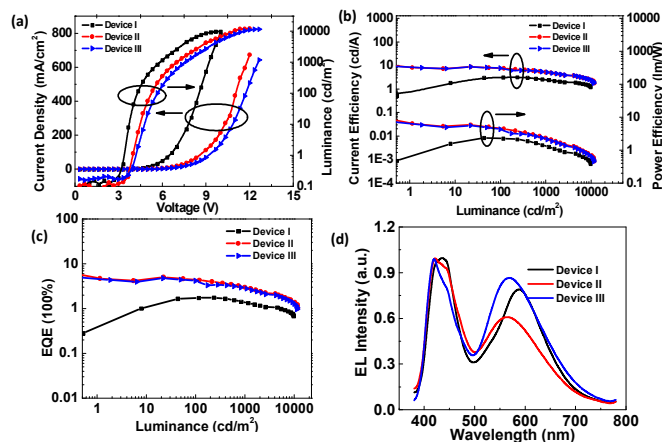


Figure 5. Electroluminescence characteristics of the WOLEDs: (a) Current density-voltage-luminance plots; (b) Current efficiency-luminance-power efficiency plots; (c) EQE-luminance plots; (d) EL spectra of the device at 6 V.

To enhance the blue emission of the devices and shift the color coordination to (0.33,0.33), Device I, II, and III are fabricated and the device structures are following: Device I: ITO/PEDOT (20 nm)/TAPC (40 nm)/TPA:mCP (5%) (5 nm)/4P-NPB:mCP (2%) (5 nm)/TmPyPB (50 nm)/LiF (0.9 nm)/Al (100 nm); Device II: ITO/PEDOT (20 nm)/TAPC (40 nm)/TPA:mCP (5%) (10 nm)/4P-NPB:mCP (2%) (10 nm)/TmPyPB (50 nm)/LiF (0.9 nm)/Al (100 nm).

nm); Device III:ITO/PEDOT (20 nm)/TAPC (40 nm)/TPA:mCP (5%) (10 nm)/mCP (5 nm)/4P-NPB:mCP (2%) (10 nm)/TmPyPB (50 nm)/LiF (0.9 nm)/Al (100 nm). As expected, all devices showed white EL emission with intense blue emission. However, the performance of Device I are obviously low: the maximum EQE of the device is only 1.8% and the emission from TXO-TPA is suppressed. This can be attributed the quenching effect of high density of triplet excitons in the narrow yellow emitting layer. Increasing the thickness of the light emitting layer, pronounced enhancement of the device performance can be observed for Device II and III. As shown in Figure 5, Device II is turned on at 4 V with a color coordination of (0.34,0.34). The maximum EQE, current efficiency, and power efficiency of the device are 4.7%, 8.1 cd/A, and 6.4 lm/W, respectively. Interestingly, low efficiency roll-off can also be observed, and the critical current density (j_c) of the device, where EQE declines by half from its peak, is about 112 mA/cm², which is higher than the reported multi-emissive layers WOLEDs based on phosphorescent emitters.¹⁸ An interlayer between the 4P-NPB:mCP and TXO-TPA:mCP layers is used to prevent mutual exciton transfer and quenching processes, which are indispensable for multi-emissive layers hybrid WOLED. Interestingly, Device III exhibits similar performance and CIE to those of Device II, indicating that the mutual quenching between 4P-NPB and TXO-TPA can be unconsidered, even mCP is not a bipolar host of 4P-NPB.

Table 2. Electroluminescence characteristics of the WOLEDs with different device structures (device I, II and III).

Device Structure	Maximum Values				Color Coordinate at 6 V
	Turn-on Voltage (V)	Current Efficiency (cd/A)	Power Efficiency (lm/W)	EQE (%)	
Device I	3.6	3.2	2.4	1.8%	(0.35,0.32)
Device II	4.0	8.1	6.4	4.7%	(0.34,0.34)
Device III	4.3	8	5.8	4.4%	(0.37,0.36)

Conclusions

In summary, a high efficiency warm white OLED with a blue fluorescent 4P-NPB emitter and yellow TXO-TPA TADF emitter was developed and showed high maximum quantum efficiency of 4.4% and stable EL spectrum with a color coordinate of (0.37,0.42). The color coordinate can be tuned to pure white by the optimization of the device structure. WOLED with color coordinate of (0.34,0.34) affords a maximum EQE of 4.7%, a current efficiency of 8.1 cd/A, and a power efficiency of 6.4 lm/W. The WOLED exhibited less pronounced efficiency roll-off with j_c of 112 mA/cm², which is highest among the pure fluorescent WOLEDs. This method opens a new alternative for achieving high performance pure fluorescent WOLEDs with simple structure.

Acknowledgments

This work was financially supported by the “Hundred Talents Program” of the Chinese Academy of Sciences, the National Natural Science Foundation of China (Grant No. 61420106002, No. 61178061, No.51373189 and No.61227008), the National Basic Research Program of China (973) (No. 2014CB932600), and the Start-Up Fund of the Technical Institute of Physics and Chemistry, the Chinese Academy of Sciences.

Notes and references

^a Key Laboratory of Photochemical Conversion and Optoelectronic Materials, Technical Institute of Physics and Chemistry, Chinese Academy of Sciences, Beijing, 100190, China.

^b Key Laboratory of Photochemical Conversion and Optoelectronic Materials and CityU-CAS Joint Laboratory of Functional Materials and Devices, Technical Institute of Physics and Chemistry, Chinese Academy of Sciences, Beijing, 100190, China.

^c University of Chinese Academy of Sciences, Beijing, 100049, China.

^d Soochow University, Jiangsu Province, China.

† Electronic Supplementary Information (ESI) available: Materials, device fabrication and characterization. See DOI: 10.1039/c000000x/

- J. Kido, M. Kimura, K. Nagai, *Science* 1994, **267**, 1332.
- S. Reineke, F. Lindner, G. Schwartz, N. Seidler, K. Walzer, B. Lüssem, K. Leo, *Nature* 2009, **459**, 234.
- Y. Sun, N. C. Giebink, H. Kanno, B. Ma, M. K. Thompson, S. R. Forrest, *Nature* 2006, **440**, 908.
- L. Ying, C.-L. Ho, H. Wu, Y. Cao, W.-Y. Wong, *Adv. Mater.* 2014, **26**, 2459.
- E. Mondal, W.-Y. Hung, H.-C. Dai, K.-T. Wong, *Adv. Funct. Mater.* 2013, **23**, 3096.
- S.-L. Lai, W.-Y. Tong, S. C. F. Kui, M.-Y. Chan, C.-C. Kwok, C.-M. Che, *Adv. Funct. Mater.* 2013, **23**, 5168.
- Y.-L. Chang, Y. Song, Z. Wang, M. G. Helander, J. Qiu, L. Chai, Z. Liu, G. D. Scholes, Z. Lu, *Adv. Funct. Mater.* 2013, **23**, 705.
- M. C. Gather, A. Köhnen, K. Meerholz, *Adv. Mater.* 2011, **23**, 233.
- H. Sasabe, J. Takamatsu, T. Motoyama, S. Watanabe, G. Wagenblast, N. Langer, O. Molt, E. Fuchs, C. Lennartz, J. Kido, *Adv. Mater.* 2010, **22**, 5003.
- L. Duan, D. Zhang, K. Wu, X. Huang, L. Wang, Y. Qiu, *Adv. Funct. Mater.* 2011, **21**, 3540.
- H. Uoyama, K. Goushi, K. Shizu, H. Nomura, C. Adachi, *Nature* 2012, **492**, 234.
- B. S. Kim, K. S. Yook, J. Y. Lee, *Sci. Rep.* 2014, **4**, 6019.
- S. Y. Lee, T. Yasuda, Y. S. Yang, Q. Zhang, C. Adachi, *Angew. Chem.* 2014, **126**, 6520.
- T. Higuchi, H. Nakanotani, C. Adachi, *Adv. Mater.* 2015, DOI: 10.1002/adma.201404967.
- H. Wang, L. Xie, Q. Peng, L. Meng, Y. Wang, Y. Yi, P. Wang, *Adv. Mater.* 2014, **26**, 5198.
- Y.-H. Lan, C.-H. Hsiao, P.-Y. Lee, Y.-C. Bai, C.-C. Lee, C.-C. Yang, M.-Y. Leung, M.-K. Wei, T.-L. Chiu, J.-H. Lee, *Org. Electron.* 2011, **12**, 756.
- S. Hofmann, T. C. Rosenow, M. C. Gather, B. Lüssem, K. Leo, *Phys. Rev. B* 2012, **85**, 245209.
- N. Sun, Q. Wang, Y. Zhao, Y. Chen, D. Yang, F. Zhao, J. Chen, D. Ma, *Adv. Mater.* 2014, **26**, 1617.